Theory of resonant multiphoton ionization of krypton by intense ultraviolet laser radiation

X. Tang and P. Lambropoulos
Department of Physics, University of Southern California, Los Angeles, California 90089-0484

Anne L'Huillier
Service de Physique des Atomès et des Surfaces, Centre d'Etudes Nucleaires de Saclay, F-91191 Gif-sur-Yvette CEDEX, France

S. N. Dixit
Lawrence Livermore Laboratory, L421 Livermore, California 94550
(Received 22 May 1989)

We present a theoretical interpretation of the experimental results on three-photon-resonant four-photon ionization of Kr reported by Landen, Perry, and Campbell [Phys. Rev. Lett. **59**, 2558 (1987)] and Perry and Landen [Phys. Rev. A **38**, 2815 (1988)]. Our calculations are based on multichannel quantum-defect theory combined with a density-matrix formalism describing the spatiotemporal development of the process. We obtain good agreement with the data, which even at intensities as high as 10^{14} W/cm^2 show the imprint of the underlying atomic structure.

I. INTRODUCTION

In two recent papers Landen, Perry, and Campbell[1] and Perry and Landen[2] have reported three-photon-resonant four-photon ionization of Kr through excited states of the type $4p^5 4d\,[\frac{3}{2}]_1$, $4p^5 4d'[\frac{5}{2}]_3$, and $4p^5 5d\,[\frac{1}{2}]_1$, at fairly high intensity, ranging from 3×10^{12} to almost 10^{14} W/cm^2. The data exhibited clear and prominent resonant enhancement which seems a bit surprising in view of the high intensity and the long-held assumption that atomic structure is obliterated at such, if not lower, intensity. More remarkable than the resonance itself is the fact that, by fitting the data to a system of amplitude equations, the authors were able to determine atomic parameters such as photoionization cross sections and ac Stark shifts for the excited states, as well as the three-photon transition strengths (Rabi frequencies) coupling the ground to the excited states. Although the experiment was elegantly designed and performed, one may wonder whether the resonance formalism employed in the fitting of the data, or even the notion of the cross section, remain meaningful and valid at these intensities and relatively short pulses (2 ps). As usual, the most direct answer to these questions comes from the comparison of the parameters extracted from the experiment with independently calculated theoretical values; a point also noted by the authors of Ref. 1. Conversely, such experimental data provide valuable information against which calculations of multiphoton parameters for such complex atoms can be tested. Our purpose in this paper is to provide such theoretical input and comparison.

II. THEORETICAL FRAMEWORK

In the course of other work, we have recently completed an elaborate analysis based on multichannel quantum-defect theory (MQDT) which makes feasible the calculation of the above parameters. Our analysis—the details of which have been published elsewhere[3]— has included bound and autoionizing states of angular momentum $J=0,1,2,3$ which enable us to construct the wave functions necessary for the calculation of all of the parameters entering the description of the process. In addition to calculating the matrix elements of the dipole operator $\epsilon\cdot\mathbf{r}$ (where ϵ is the polarization vector of the radiation) required in all of the above parameters, the ac Stark shifts and the three-photon Rabi frequencies require the performance of the summation over complete sets of intermediate states; a single summation for the ac Stark shifts and a double summation for the three-photon Rabi frequencies. In the MQDT formalism employed here, these summations have been performed through the truncated contribution of a finite number of terms. As usual in this type of calculation[4]—excepting those rare cases, like hydrogenic systems in which the exact Green's function is known—one has to choose between an infinite summation of more or less approximate matrix elements and a truncated summation of much more accurate terms. The limitations and strengths of the approach adopted here have been discussed in Ref. 3. Although by no means exact, our results in this paper should not be off by more than a factor of 2. Since the preparation of our manuscript for the work of Ref. 3, we have had the opportunity to test calculations based on our MQDT analysis in various contexts such as ac Stark shifts,[5] photoelectron angular distributions,[6] as well as harmonic generation,[7] with results that lend confidence to the framework of our analysis, although refinements will surely be necessary.

Aside from the need for realistic atomic parameters, the derivation of theoretical resonance line shapes requires the solution of the density-matrix equations appropriate to this $3+1$ process, including the realistic temporal and spatial distribution of the laser intensity. As discussed in more detail below, the experiment of Landen, Perry, and Campbell[1] may have involved the simultaneous excitation of two resonances. We therefore show

here the set of density-matrix equations corresponding to that more general case, as employed in our calculations. Obviously, the case of one intermediate resonance is obtained from the two-resonance model as a special case.

Let $|g\rangle$ be the ground and $|a\rangle, |b\rangle$ the excited atomic states with respective energies $\hbar\omega_g$, $\hbar\omega_a$, and $\hbar\omega_b$. The frequency of the laser is denoted by ω and the polarization by ϵ, which for light linearly polarized, as in this experiment, is taken along the z axis. The electric field is then written as $E\epsilon\cos(\omega t)$. The differential equations for the slowly varying elements $\sigma_{ij}(t)$ $(i,j=g,a,b)$ of the density matrix $\rho(t)$ can be written as

$$\frac{d}{dt}\sigma_{gg}=\mathrm{Im}(\Omega_{ga}\sigma_{ag}+\Omega_{gb}\sigma_{bg}) , \tag{1}$$

$$\frac{d}{dt}\sigma_{aa}=-\Gamma_a\sigma_{aa}-\mathrm{Im}(\Omega_{ga}\sigma_{ag}-\Omega_{ab}^{*}\sigma_{ab}) , \tag{2}$$

$$\frac{d}{dt}\sigma_{bb}=-\Gamma_b\sigma_{bb}-\mathrm{Im}(\Omega_{gb}\sigma_{bg}+\Omega_{ab}\sigma_{ab}) , \tag{3}$$

$$\left[\frac{d}{dt}-i\Delta_a+\tfrac{1}{2}\Gamma_a\right]\sigma_{ag}=\tfrac{1}{2}i\Omega_{ag}(\sigma_{aa}-\sigma_{gg})-\tfrac{1}{2}i\Omega_{ab}\sigma_{bg}+\tfrac{1}{2}i\Omega_{bg}\sigma_{ab} , \tag{4}$$

$$\left[\frac{d}{dt}-i\Delta_0+\tfrac{1}{2}\Gamma_b\right]\sigma_{bg}=\tfrac{1}{2}i\Omega_{bg}(\sigma_{bb}-\sigma_{gg})-\tfrac{1}{2}i\Omega_{ba}\sigma_{ag}+\tfrac{1}{2}i\Omega_{ag}\sigma_{ba} , \tag{5}$$

$$\left[\frac{d}{dt}+i\bar{\omega}_{12}+\tfrac{1}{2}(\Gamma_a+\Gamma_b)\right]\sigma_{ab}=-\tfrac{1}{2}i\Omega_{ag}\sigma_{gb}+\tfrac{1}{2}i\Omega_{gb}\sigma_{ag}+\tfrac{1}{2}i(\Omega_{ab}^{*}\sigma_{aa}-\Omega_{ab}\sigma_{bb}) , \tag{6}$$

where the transformation $\sigma_{ij}(t)=\rho_{ij}(t)e^{-i3\omega t}$ has removed the rapid (resonant) time variation of those off-diagonal matrix elements that connect the ground with each of the resonant (or near-resonant) excited states. Off-diagonal matrix elements between the excited states themselves involve two-photon virtual transitions similar to those occurring in the calculation of ac Stark shifts. They are not usually found in theoretical treatments of problems involving more than one resonant state in the same transition; they can, however, be of quantitative importance if the circumstances are appropriate, as we have shown in other contexts.[8] It is only after quantitative evaluation of their contribution that they can be neglected as has been the case here.

Ω_{ga} and Ω_{gb} are the three-photon Rabi frequencies coupling the state $|g\rangle$ to $|a\rangle$ and $|b\rangle$, respectively. They are given by $E^3\mu^{(3)}$ with $\mu^{(3)}$ being the corresponding three-photon effective electric dipole matrix element[3] including radial as well as angular momentum contributions and all multiplicative constants. Γ_a and Γ_b represent the ionization widths of the respective states, given by the product $\hat{\sigma}F$ of the respective (single-photon) ionization cross section σ and the photon flux F. The detuning from resonance with the intermediate state $|j\rangle$ $(j=a,b)$ is $\Delta_j=3\omega-\bar{\omega}_{jg}$ where all atomic energy differences (in units of rad/s) of the type $\bar{\omega}_{jg}=\bar{\omega}_j-\bar{\omega}_g$ $(j=a,b)$ bear a horizontal bar to indicate that the ac Stark shift S_j or S_g has been added to the respective free-atom energy. These shifts are proportional to the laser intensity I (W/cm^2). All of the above atomic parameters are time dependent on a time scale over which the intensity $I(t)$ varies; a time variation slow compared to $2\pi/\omega$. As a consequence, the differential equations (1)–(4) have time-dependent coefficients.

Since the experiments measured the amount of ionization as reflected in the number of ions generated, the observed signal is represented by the quantity

$$P_{\mathrm{ion}}(T_L)=1-\sigma_{gg}(T_L)-\sigma_{aa}(T_L)-\sigma_{bb}(T_L) , \tag{7}$$

where T_L indicates that the differential equations have been integrated over the duration and shape of the laser pulse. The quantity $P_{\mathrm{ion}}(T_L)$ must in addition be integrated over the volume of interaction defined by the lens system focusing the laser radiation. We need not describe the details of these procedures here as we have employed the spatiotemporal distribution specified by Perry and Landen.[2] We do note, however, that our calculations provide the absolute amount of ionization produced during the pulse and integrated over the volume of interaction as specified in Ref. 2. All saturation effects are therefore automatically included in our results. In fact, the severe broadening present at higher intensities, in all of our figures, is the result of saturation.

We should perhaps mention here that the wave functions employed in the calculations contain many coupled channels, representing combinations of the two fine-structure states of the ion and the different angular momentum states of the excited electron in a three-photon transition. The frequency employed in the experiments was such that $4\hbar\omega$ was larger than the second ionization threshold $[P_{1/2}]$. As a result, the measured signal contained ions in both angular momentum states, $[P_{3/2}]$ and $[P_{1/2}]$, with a branching ratio depending on the resonant state. Although this ratio is obtained as part of our calculation, we have no corresponding experimental quantity for comparison.

The shift observed in the experiment is determined by

the difference between the shift of the excited and that of the ground state which is much smaller than that of the excited state. The calculated values we quote represent the difference which can be compared to the experimental values.

III. RESULTS AND DISCUSSION

A. Atomic parameters

For each of the resonant excited states, the fitting of the experimental data to a set of equations similar to—strictly speaking, a special case of—ours has yielded three parameters for each resonance. In Table I we list the experimental[2] together with our calculated values. For reasons discussed below, we show calculated values for three excited states, while Perry and Landen[2] show values for two.

Consider the state $4d[\frac{3}{2}]_1$ first. Theory and experiment are in excellent agreement for the ac Stark shift and the three-photon Rabi frequency. There is a discrepancy of a factor of 2 for the photoionization cross sections. Given the quoted experimental error of about 12% and the fact that we would not place better than 50% confidence on our theoretical value, the discrepancy is of no particular significance.

We turn now to the other resonances identified by Perry and Landen[2] as $4d'[\frac{5}{2}]_3$, in contrast to their earlier[1] identification as $5d[\frac{1}{2}]_1$. The ambivalence is quite understandable since these two states are (in the free atom) separated by 100 cm^{-1}) while their widths at an intensity of 10^{13} W/cm^2 are of the order of 1000 cm^{-1}. Given that a pulse rises to a peak value and falls, one cannot say that the resonances were overlapping completely, but they would certainly influence each other as we illustrate below. Theory gives us a set of parameters for each of these states as listed in Table I. Although direct comparison of either set of these parameters with the experimental values is not completely meaningful, we note that they agree much more than one might have expected, in view of the simultaneous presence of two resonances.

B. Theoretical resonance line shapes

For the $4d[\frac{3}{2}]_1$ resonance, we expect the calculated line shapes to be quite similar to those of the experiment,

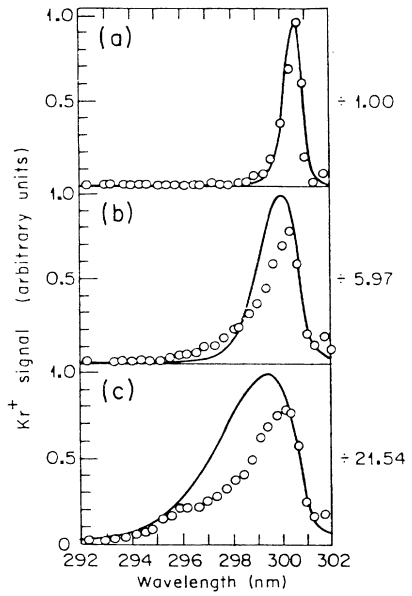

FIG. 1. Spectral profile of resonance $4d[\frac{3}{2}]_1$, for various peak intensities (a) $I_0=5.8\times10^{12}$ W/cm^2, (b) $I_0=1.4\times10^{13}$ W/cm^2, (c) $I_0=2.8\times10^{13}$ W/cm^2. Solid curves are the results of calculations as described in the text. Circles are the experimental data. Theory is normalized to the data at the lowest reported intensity. The numbers to the right of the figure frames represent the ratio of ionization to that of frame (a). The corresponding experimental values were 1:4.6:16.5. These experimental values were communicated to us by Perry and Landen (Ref. 9). Note that the corresponding numbers given in Fig. 15 of Ref. 2 represent ratios of areas and not of peak heights, while those in Fig. 14 of Ref. 2 represent ratios of peak heights.

given that the two sets of parameters are so close to each other. Whatever differences emerge are due to the small differences between theoretical and experimental parameters. We show the calculated line shapes plotted against the experimental data in Fig. 1. Since the experiment does not provide an absolute calibration of the amount of ionization, we have normalized our theory to the experimental points at the lowest intensity. We note a small departure of the theory from the data at the higher inten-

TABLE I. Comparison of atomic parameters deduced from the experiment with those obtained from the theory. The values of the photoionization cross sections are given in units of cm^2, those of the shifts in $cm^{-1}/(10^{13}$ $W/cm^2)$, and those of the Rabi frequencies in rad/s if the value of I is inserted in units of W/cm^2.

Excited state	Photoionization cross section		ac Stark shift		Three-photon Rabi frequency	
	Expt.	Theory	Expt.	Theory	Expt.	Theory
$4d[\frac{3}{2}]_1$	8×10^{-18}	3.9×10^{-18}	639	643	$1.7\times10^{-7}I^{3/2}$	$1.21\times10^{-7}I^{3/2}$
$4d'[\frac{5}{2}]_3$	3×10^{-18}	10.6×10^{-18}	314	556	$7.8\times10^{-8}I^{3/2}$	$3.1\times10^{-8}I^{3/2}$
$5d[\frac{1}{2}]_1$		5.6×10^{-18}	756			$1.9\times10^{-9}I^{3/2}$

sities. Whether this is due to errors in the theoretical values or to the fact that, at higher intensities, the shape becomes much more sensitive to spatiotemporal parameters, or both, remains to be seen. The fact that the theoretical maximum of ionization increases a bit faster than the experimental is compatible with the smaller theoretical value of the ionization cross section which will tend to cause less broadening. Given, however, that many parameters play a role, this should be viewed only as an indication.

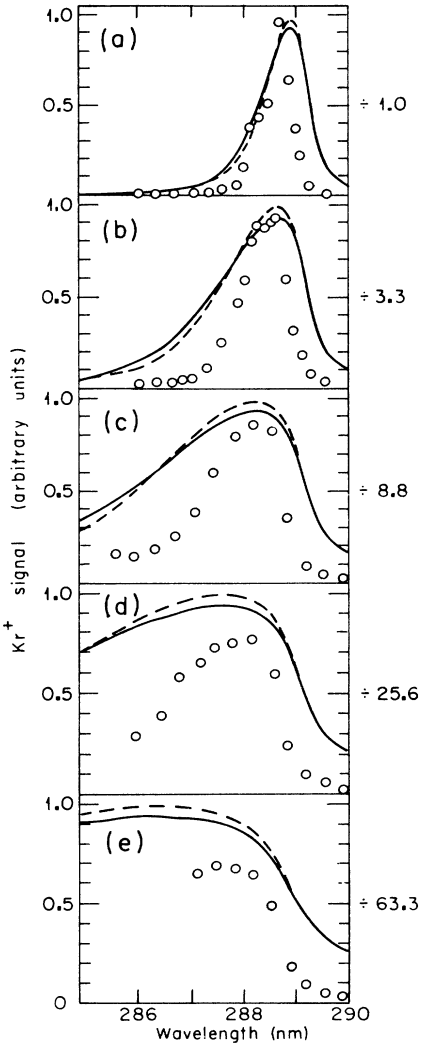

FIG. 2. Spectral profile of resonances $4d'[\frac{5}{2}]_3$ and $5d[\frac{1}{2}]_1$ for various peak intensities. (a) $I_0=7.4\times10^{12}$ W/cm^2, (b) $I_0=1.5\times10^{13}$ W/cm^2, (c) $I_0=2.7\times10^{13}$ W/cm^2, (d) $I_0=4.5\times10^{13}$ W/cm^2, (e) $I_0=7.8\times10^{13}$ W/cm^2. Solid curves correspond to the calculation with both resonant states, while dashed curves correspond to the calculation which includes only state $4d'[\frac{5}{2}]_3$. Theory is normalized as in Fig. 1. The corresponding experimental values of the ratios were 1:3.1:7.8:18.6:43.5.

For the other resonances, theory dictates that we calculate the line shape including both resonant states $4d'[\frac{5}{2}]_3$ and $5d[\frac{1}{2}]_1$ because we know that they will influence each other. The result is shown in Fig. 2 together with the experimental data. We see again that, with increasing intensity, the maximum of the theoretical curve rises above that of the data. At the highest of the intensities in Fig. 2, the theoretical maximum is a bit less than 50% above the experimental one. In the same figure, we have also plotted theoretical line shapes calculated with only one of the resonances, namely, $4d'[\frac{5}{2}]_3$, included. The main purpose of this additional plot is to show the sensitivity (or lack of it) of the line shape to the presence of the other resonance. Clearly, the $4d'$ makes the dominant contribution which is compatible with its higher Rabi frequency (see Table I). To complete the comparison, we show in Fig. 3 the line shapes resulting from a calculation which includes only state $5d[\frac{1}{2}]_1$ as resonance. This is the state adopted as the primary resonance by Landen, Perry, and Campbell in their earlier pa-

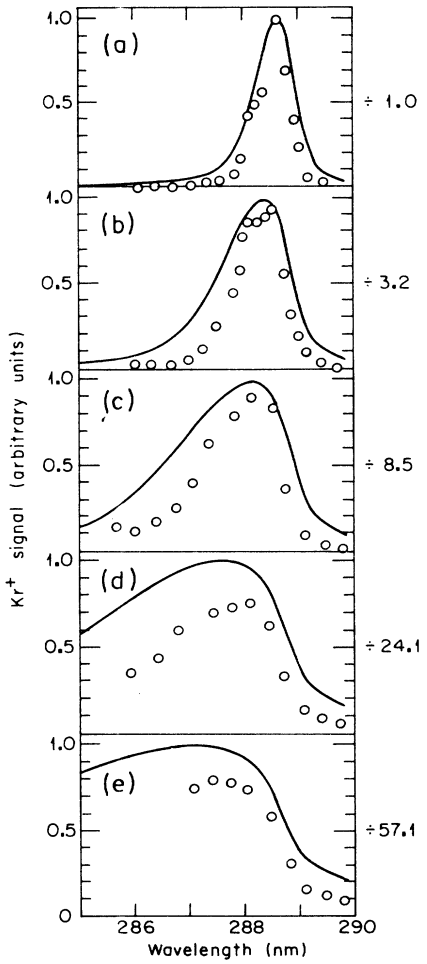

FIG. 3. Same as Fig. 2, but with only state $5d[\frac{1}{2}]_1$ included in the calculation.

per.[1] The experimental data are shown again in Fig. 3. Again, we note a small departure of theory from experiment at the higher intensities. Curiously, this theoretical line shape is a bit closer to the data, but the difference from Fig. 2 is too small to be given much significance.

In conclusion, we note that the atomic parameters obtained from the independent theoretical calculation are in very good agreement with those deduced from the experiment. This agreement leaves no doubt about the imprint of atomic structure on this and related high-intensity laser interactions with atoms. The differences between theoretical and experimental parameters are easily understood in view of the complexity of both experiment and theory. The resulting discrepancies in the line shapes, which are to be expected in view of the differences in the values of the parameters, provide a good illustration of the role of the spatiotemporal distribution of intensity in such high-intensity studies. Hopefully, further comparisons between theory and experiment will shed more light upon the intricate interplay of the various processes leading to a resonance line shape. They will also provide a basis for the refinement of theoretical multiphoton parameters.

ACKNOWLEDGMENTS

This work was supported by the National Science Foundation Grant No. PHY-8609966. Work done by S.N.D. was performed under the auspices of the U.S. Department of Energy by Lawrence Livermore National Laboratory under Contract No. W-8405-ENG-48.

[1]O. L. Landen, M. D. Perry, and E. M. Campbell, Phys. Rev. Lett. **59**, 2558 (1987).

[2]M. D. Perry and O. L. Landen, Phys. Rev. A **38**, 2815 (1988).

[3]Anne L'Huillier, X. Tang, and P. Lambropoulos, Phys. Rev. A **39**, 1112 (1989).

[4]P. Lambropoulos, Adv. At. Mol. Phys. **12**, 87 (1976).

[5]A. L'Huillier, L. A. Lompré, D. Normand, M. Ferray, X. Tang, and P. Lambropoulos, J. Opt. Soc. Am. B (to be published).

[6]R. N. Compton and S. Bajic (private communication and unpublished); D. Charalambidis, B. H. Feng, and C. Fotakis (unpublished).

[7]M. J. Proctor, J. A. D. Stockdale, T. Efthimiopoulos, and C. Fotakis, Chem. Phys. Lett. **137**, 223 (1987); X. Tang and P. Lambropoulos (unpublished).

[8]S. N. Dixit and P. Lambropoulos, Phys. Rev. A **27**, 861 (1983).

[9]M. D. Perry and O. L. Landen (private communication).